

Magnetite nanoparticles as smart carriers to manipulate the cytotoxicity of anticancer drugs: Magnetic control and pH-responsive release

Zhenghuan Zhao, Dengtong Huang, Zhenyu Yin, Xiaoqin Chi, Xiaomin Wang, Jinhao Gao

Supplementary Information

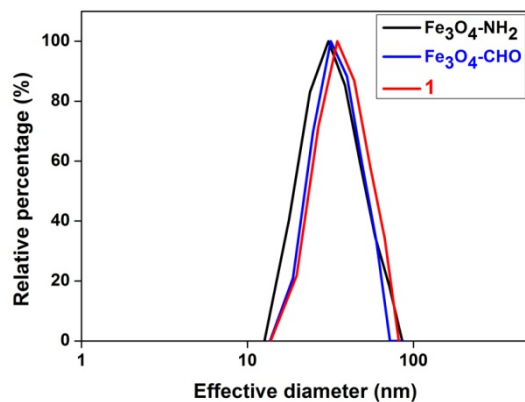


Fig. S1. DLS analysis of $\text{Fe}_3\text{O}_4\text{-NH}_2$, $\text{Fe}_3\text{O}_4\text{-NH}_2$ reacted with glutaraldehyde ($\text{Fe}_3\text{O}_4\text{-CHO}$), and nanoparticle conjugates **1**.

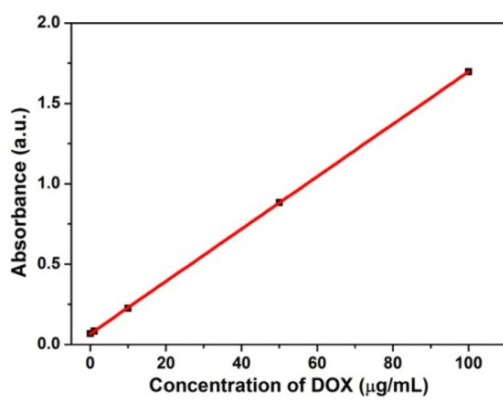


Fig. S2. Calibration curve based on UV-Vis analysis of DOX with different concentrations.

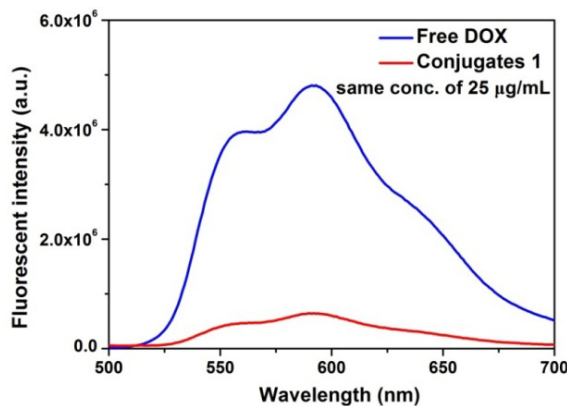


Fig. S3. Fluorescence spectra of free DOX (25 $\mu\text{g}/\text{mL}$) and nanoparticle conjugates **1**. There is fluorescence quenching in nanoparticle conjugates **1**. Excitation wavelength is 470 nm.

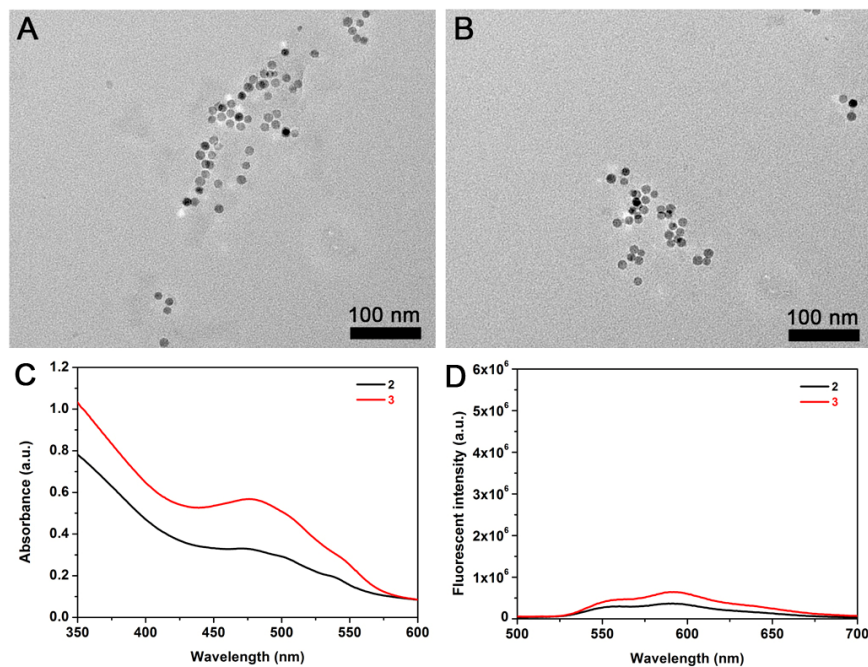


Fig. S4. TEM images of (A) nanoparticle conjugates **2** and (B) nanoparticle conjugates **3** in PBS buffer. (C) UV-Vis analysis of nanoparticle conjugates **2** and **3** in PBS buffer. (D) Fluorescence spectra of nanoparticle conjugates **2** (~15 μg DOX/mL) and **3** (~25 μg DOX/mL) in PBS buffer, showing the existence of fluorescence quenching. Excitation wavelength is 470 nm.

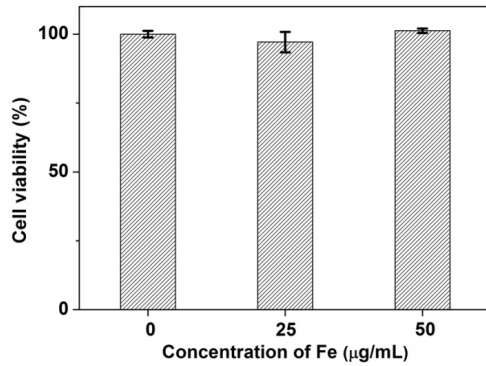


Fig. S5. MTT assay of HeLa cells treated by $\text{Fe}_3\text{O}_4\text{-NH}_2$ nanoparticles at 0, 25, and 50 $\mu\text{g}/\text{mL}$ for 24 h.

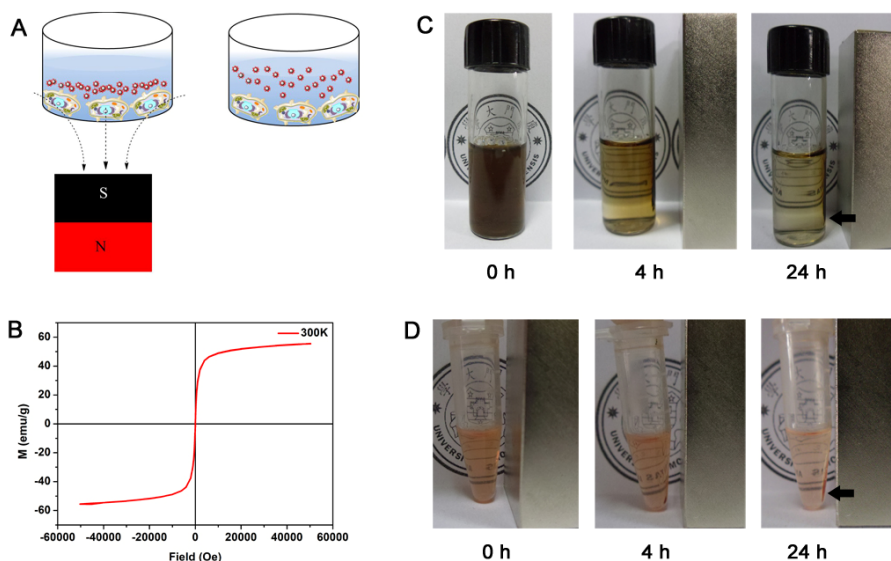


Fig. S6. (A) The schematic cartoon showing the different distribution of magnetic drug carriers with or without external magnetic fields. (B) The field-dependent magnetization M-H curve of $\text{Fe}_3\text{O}_4\text{-NH}_2$ sample at 300 K (the magnetic moment of about 55 emu/g), suggesting that the $\text{Fe}_3\text{O}_4\text{-NH}_2$ nanoparticles have response to a small magnet. Photographic images of the behaviors of (C) $\text{Fe}_3\text{O}_4\text{-NH}_2$ and (D) nanoparticle conjugates **1** with high concentrations under the magnetic fields (~3000 G), showing the increased concentration gradient of magnetic nanoparticles after 4 h and the evident accumulation of magnetic nanoparticles close to the magnets after 24 h (arrows).

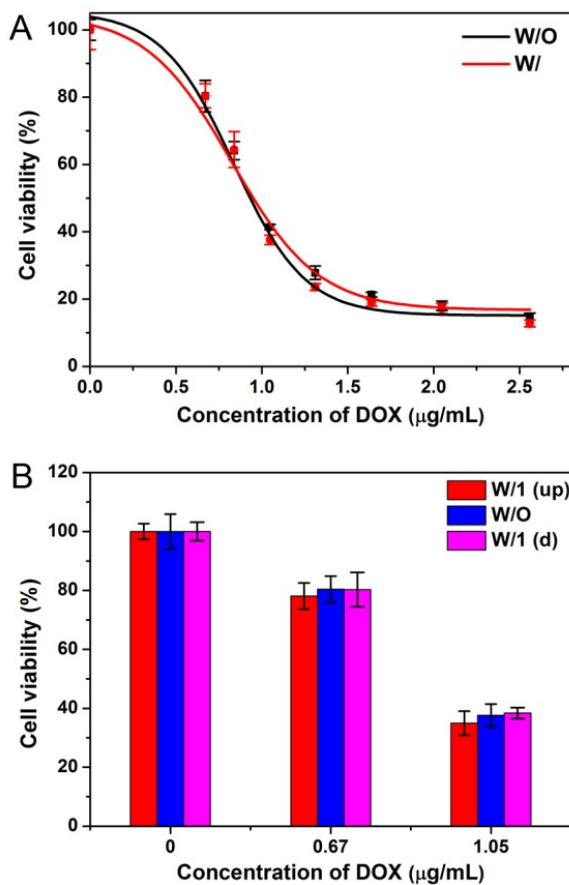


Fig. S7. (A) MTT assay (24 h) curves of HeLa cells treated by free DOX at different concentrations with and without magnetic fields (400 G). (B) MTT assay (24 h) of HeLa cells treated by free DOX at different DOX concentrations (0, 0.67, and 1.05 $\mu\text{g/mL}$, respectively) with (up or down) and without magnetic fields (1000 G). The error bars represent standard deviation of five independent experiments.

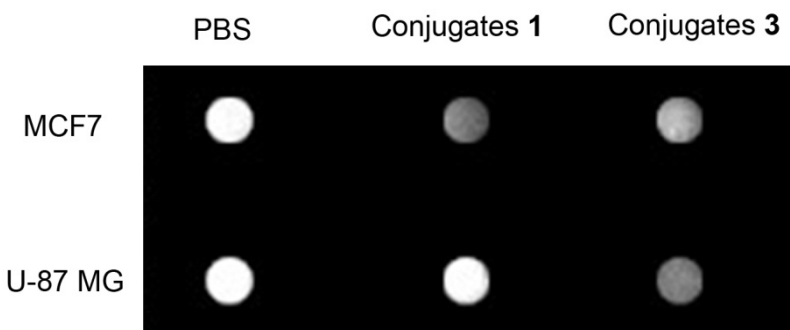


Fig. S8. T_2 -weighted MR images of MCF7 and U-87 MG cells after treated by PBS, nanoparticle conjugates **1**, and conjugates **3** for 4 h, respectively. The cellular uptake of conjugates **1** by MCF7 cells was slight higher than that of conjugates **3**, while cellular uptake of conjugates **3** by U-87 MG cells was much higher than that of conjugates **1**.

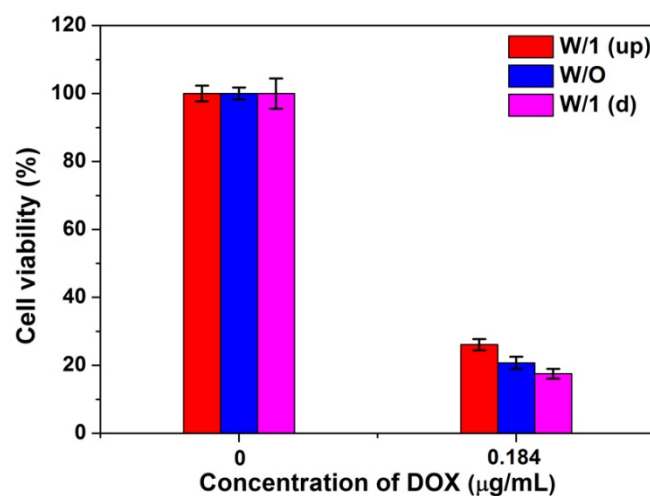


Fig. S9. MTT (24 h) assay of U-87 MG cells treated by conjugates **3** at different DOX concentrations (0 and 0.184 $\mu\text{g}/\text{mL}$, respectively) with magnetic fields (1000 G, at the top or bottom of the cell samples) and without magnetic fields. There is the obvious difference on cell toxicity because of external magnetic fields. The error bars represent standard deviation of five independent experiments.

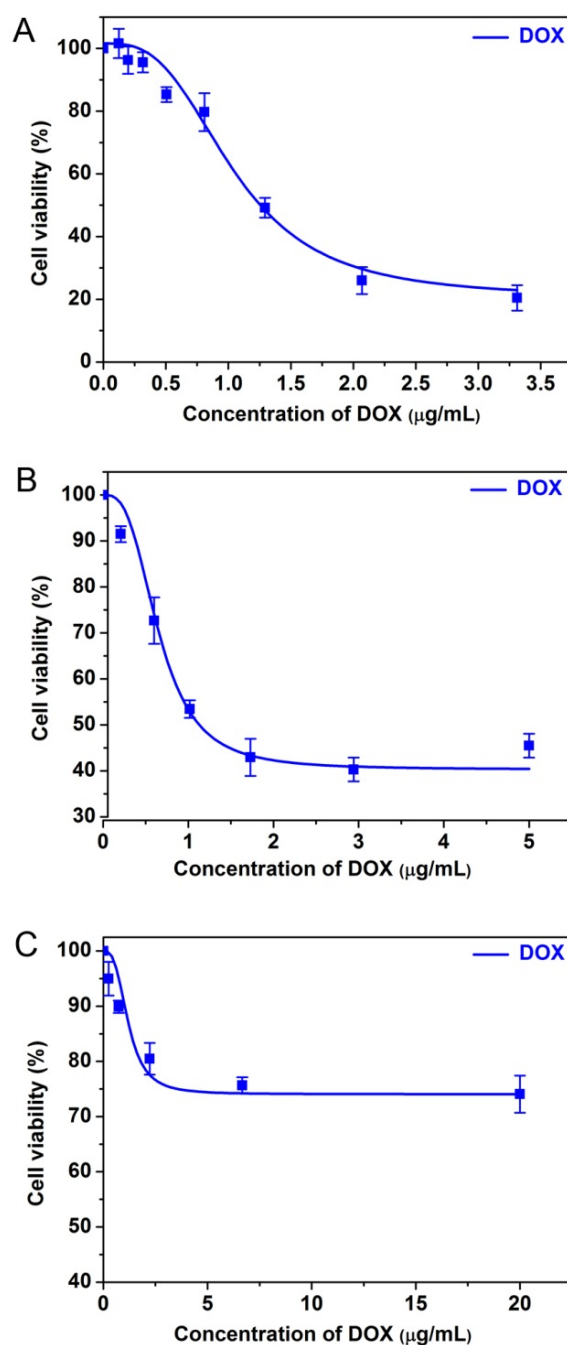


Fig. S10. MTT assay curves of (A) HeLa cells, (B) MCF7 cells, and (C) U-87 MG cells with free DOX at different concentrations for 24 h. The error bars represent standard deviation of five independent experiments.

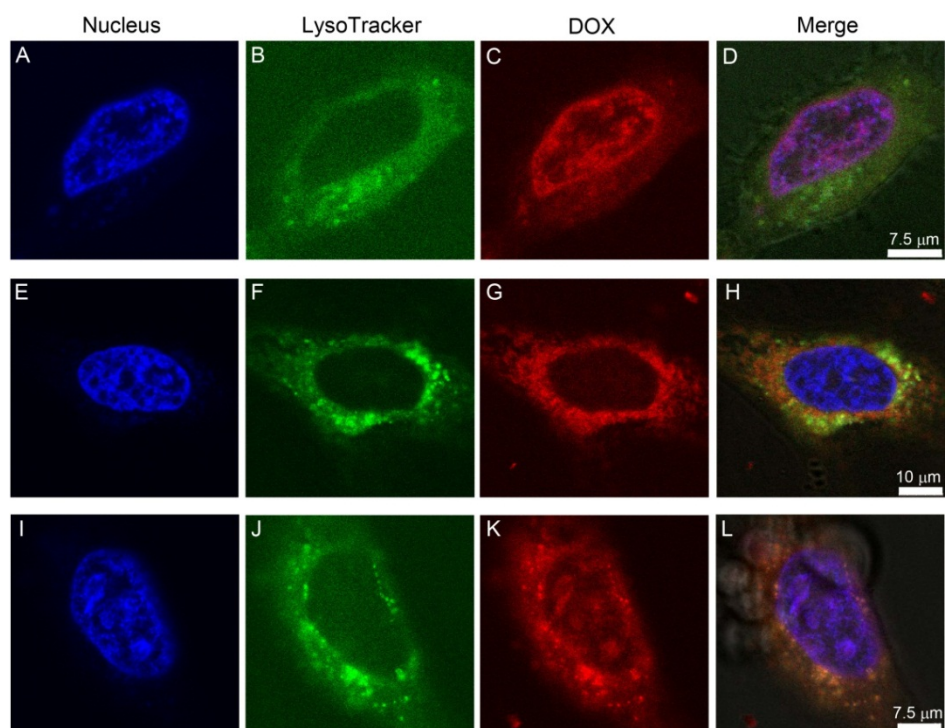


Fig. S11. Representative confocal images (high magnification) of HeLa cells after treatment with (A-D) DOX for 0.5 h. Representative confocal images (high magnification) of HeLa cells after treatment with conjugate **1** for (E-H) 0.5 h and (I-L) 4 h, respectively. Cell nuclei were stained with Hoechst 33342 (blue) and lysosomes were labeled with LysoTracker Green DND-26 (green).